

## Proton hole states in neutron rich Pd nuclei

E. R. Flynn, F. Ajzenberg-Selove,\* Ronald E. Brown, J. A. Cizewski,<sup>†</sup> and J. W. Sunier  
*Los Alamos National Laboratory, Los Alamos, New Mexico 87545*

(Received 6 December 1982)

The  $(\vec{t}, \alpha)$  reaction at 17 MeV triton energy has been used to study proton hole states in targets of  $^{106,108,110}\text{Pd}$ . The results indicate that for the residual nuclei,  $^{105,107,109}\text{Rh}$ , the ground states have a spin of  $\frac{7}{2}^+$ , in contrast to the lighter Rh nuclei, and are not of single-particle character. Coupled-channels analysis indicates a possible particle-vibration character for these ground states. A strong neutron-proton interaction may be evident from the level systematics of Rh nuclei as the ground state spins change between  $N=58$  and  $N=60$  ( $^{103}\text{Rh}$  and  $^{105}\text{Rh}$ ).

[NUCLEAR REACTIONS  $^{106,108,110}\text{Pd}(\vec{t}, \alpha)$ ,  $E=17.0$  MeV; measured  $\sigma(\theta)$ ,  $A_y$ . Deduced levels  $^{105,107}\text{Rh}$ . DWBA, CCBA analyses.]

## I. INTRODUCTION

The use of a polarized triton beam to measure the spin and spectroscopic factors of proton hole states is now well established.<sup>1-3</sup> The large analyzing powers ( $A_y$ ) together with the differential cross sections enable rather definitive spin assignments to be made, and with the use of empirical normalization factors, absolute spectroscopic factors may be obtained. In the present paper, we utilize these features to obtain information regarding the spectroscopy of neutron rich Rh nuclei. These results are part of a larger study which we are undertaking to investigate the shape transition region which appears to occur near neutron number  $N=60$  and proton numbers  $Z=38-46$ . The onset of deformation observed in this region has been proposed<sup>4</sup> to be due to a large interaction between  $g_{7/2}$  neutrons and  $g_{9/2}$  protons, which seriously affects the Fermi surface and results in abnormal level patterns. There have previously been extensive fission-fragment decay scheme measurements in this region,<sup>5</sup> as well as two-nucleon transfer studies.<sup>6</sup> A study has also been made of particle-vibration multiplets.<sup>7</sup>

The previous study of this region by the  $(\vec{t}, \alpha)$  reaction<sup>1</sup> employed the targets  $^{104}\text{Ru}$  and  $^{110}\text{Pd}$ . In the  $^{110}\text{Pd}(\vec{t}, \alpha)$  reaction it was noted that the ground-state transition is extremely weak and contains little single-particle transfer strength. The single-particle strength to the  $\frac{7}{2}^+$  ground state arises from an orbital belonging to another shell. To understand the presence of such a state, we have considered it as a particle-vibration level which has been pushed below the normal single particle orbital and is excited in

single particle transfer primarily by higher order processes. For this analysis we have performed coupled channel Born approximation (CCBA) calculations assuming excitation through inelastic scattering followed by single particle transfer in the strong channels.

The systematic behavior of the Rh isotopes through the changes in ordering of the proton levels as the neutron levels are filled provides further evidence for the importance of the dominance of a neutron-proton interaction. We therefore present the systematics using the data described here in addition to previous data on other isotopes.<sup>8</sup>

## II. EXPERIMENTAL PROCEDURES

The experiments involved the use of the 17-MeV polarized triton beam at the Los Alamos National Laboratory Van de Graaff facility, and of a quadrupole-three-dipole (Q3D) spectrometer having a one-meter, helical-cathode focal plane detector.<sup>9</sup> Details of the procedure may be found in Ref. 3. The  $^{106,108}\text{Pd}$  target thicknesses were 100 and 74  $\mu\text{g}/\text{cm}^2$ , respectively. Beam currents of 40–50 nA were used and exposures of 60  $\mu\text{C}$  were taken for each spin orientation and angle. Energy calibration of the focal plane was done using the  $^{60}\text{Ni}(t, \alpha)^{59}\text{Co}$  reaction to known levels of  $^{59}\text{Co}$ . Angular distributions were taken from  $10^\circ$  to  $45^\circ$  in  $5^\circ$  steps. The  $^{110}\text{Pd}$  experiment is described in Ref. 1.

## III. RESULTS

Spectra for the  $^{106}\text{Pd}(\vec{t}, \alpha)^{105}\text{Rh}$  and  $^{108}\text{Pd}(\vec{t}, \alpha)^{107}\text{Rh}$  reactions are shown in Figs. 1 and

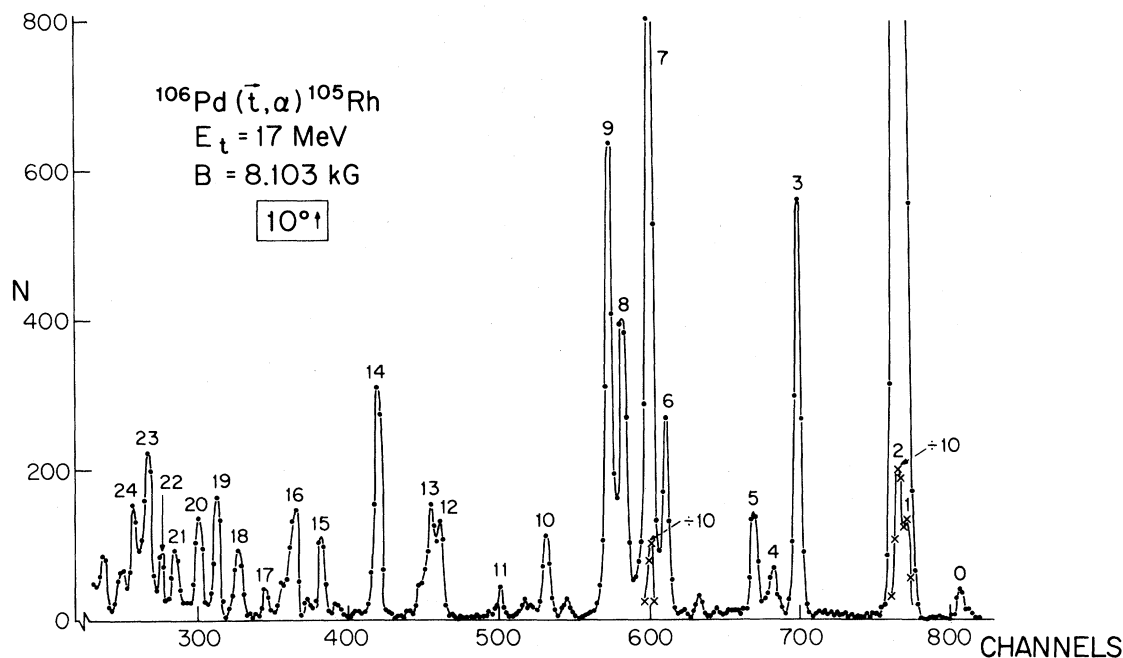


FIG. 1. Spin up spectrum of the  $^{106}\text{Pd}(\vec{t}, \alpha)^{105}\text{Rh}$  reaction at  $10^\circ$ .  $N$  represents the total number of counts in a two channel bin.

2, respectively. We also include in Fig. 3 a spectrum of the  $^{110}\text{Pd}(t, \alpha)^{109}\text{Rh}$  data discussed in Ref. 1, because it was incorrectly presented there (see the erratum of Ref. 1). Tables I and II present the  $^{105,107}\text{Rh}$  results and compare them with previous data on these isotopes. In the case of  $^{107}\text{Rh}$  there were previously few spin assignments. In neither case have

there been previous single proton pickup experiments. The angular distributions of differential cross sections and  $A_y$  are shown in Figs. 4 and 5, respectively, for those levels of  $^{105,107}\text{Rh}$  which were excited with sufficient strength. The spin assignments given in Tables I and II are based on both the empirical shapes of  $A_y$  and  $d\sigma/d\Omega$  as well as on dis-

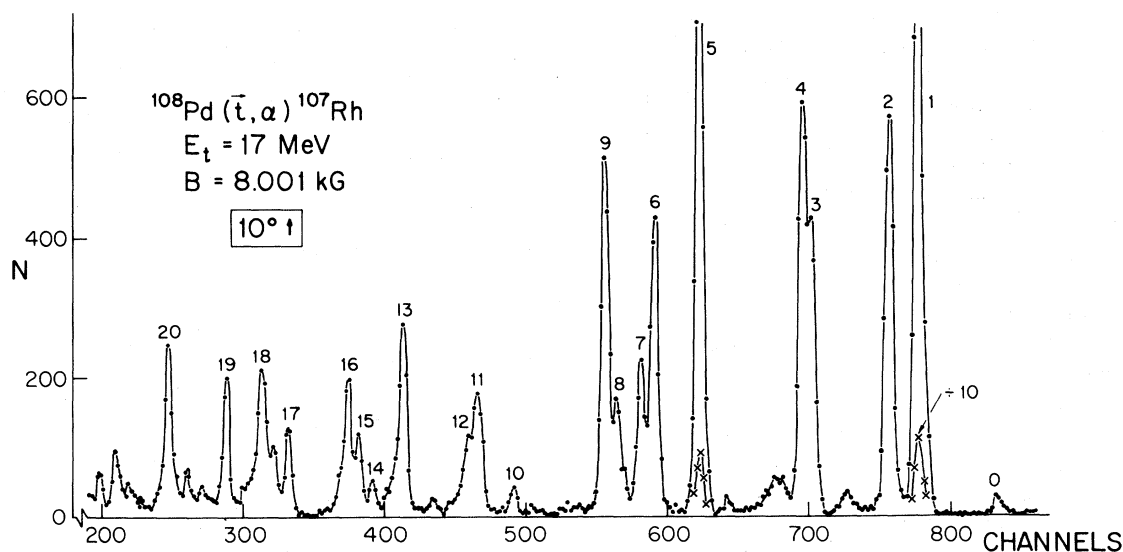


FIG. 2. Spin up spectrum of the  $^{108}\text{Pd}(\vec{t}, \alpha)^{107}\text{Rh}$  reaction at  $10^\circ$ . See also the caption of Fig. 1.

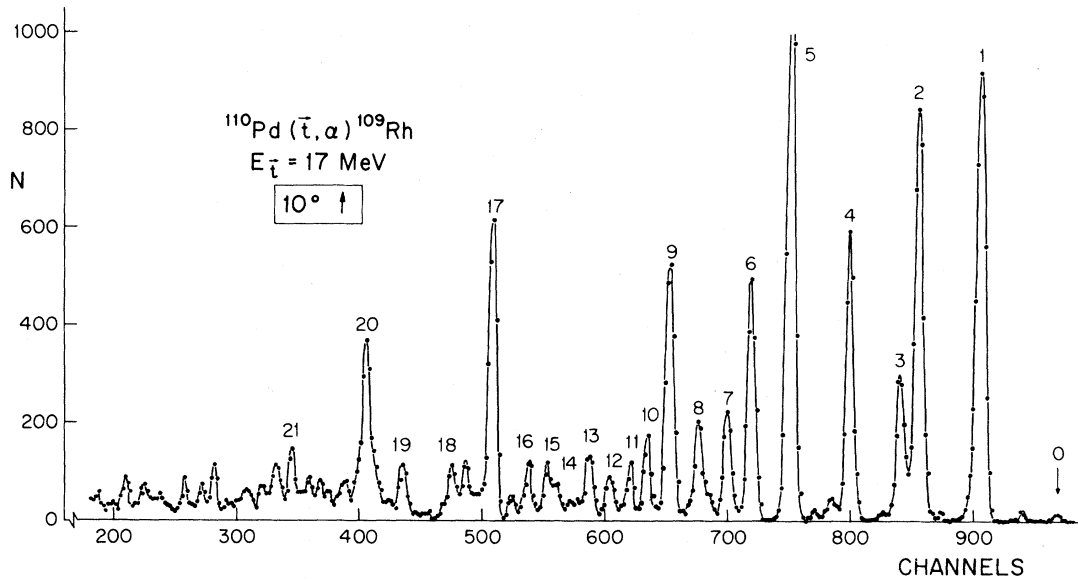


FIG. 3. Spin up spectrum of the  $^{110}\text{Pd}(\vec{t}, \alpha)^{109}\text{Rh}$  reaction at  $10^\circ$  measured in Ref. 1. The group at channel  $\sim 940$  is due to the 754 keV state in  $^{107}\text{Rh}$ . See also the caption of Fig. 1.

torted wave (DW) calculations discussed in Sec. IV. We have tried to limit these assignments to states that are sufficiently excited to be considered as having been populated by direct processes. However, as we discuss in Sec. IV, states considered to be excited by strong channel coupling processes, such as the  $\frac{7}{2}^+$  ground states, also appear to give correct spin signatures.

#### IV. DISTORTED WAVE CALCULATIONS

Two types of distorted wave calculations were performed for the present data. First, we carried out calculations using the zero range single channel code DWUCK4 of Kunz.<sup>10</sup> It was shown previously<sup>1</sup> that the angular distributions of differential cross sections and  $A_y$  of most states excited in the  $(\vec{t}, \alpha)$  reaction can be described accurately by this procedure as long as they have reasonable strength. The optical-model parameters used in the DW calculations were the same as in Ref. 1, with a normalization factor of 11.6 being used again for consistency. The resulting spectroscopic factors are shown in Tables I and II. In Table III we summarize the energies and spectroscopic values of the states which carry the principal single particle strength to show the systematic trends.

The weak excitation of the  $\frac{7}{2}^+$  ground states found in the Rh nuclei examined here and in Ref. 1 arises from an orbital not found in the proton shell below  $Z=50$ . In order to understand more fully the

excitation of these states, the coupled channel code DWUCK5 (Ref. 11) of Kunz was used. The coupling was done as shown in Fig. 6. The excitation energies of the  $2^+$  state in the even Pd core as well as the deformation  $\beta$  values, were taken from the literature.<sup>8</sup> The spectroscopic factor and excitation energy of the  $\frac{9}{2}^+$  state are from the present results. The calculations for the ground state transitions to the  $\frac{7}{2}^+$  states of  $^{105,107,109}\text{Rh}$  are shown in Fig. 7. The calculation gives the correct cross section for the  $\frac{7}{2}^+$  ground states to within 20%, assuming a spectroscopic factor for  $g_{7/2}$  transfer  $S_{7/2}=0.1$  and a direct transfer phase for the  $\frac{7}{2}^+$  particle opposite to that for the  $\frac{9}{2}^+$  particle. The  $g_{9/2}$  transfers from the ground state to the  $\frac{9}{2}^+$  state, and from the  $2^+$  state to the final  $\frac{7}{2}^+$  or  $\frac{5}{2}^+$  states, were assumed to have a DWBA spectroscopic strength of 3.7 and equal phases. The value  $S_{7/2}=0.1$  reproduces the observed transition strength, with values below this having only a small effect on the cross section but still having an appreciable effect on the analyzing power. The  $C^2S$  values for the  $\frac{7}{2}^+$  ground states given in parentheses in Tables I and II are from DWBA calculations. The fact that they are larger than the value of 0.1 used in the CCBA calculations reflects the importance of coupled-channel effects for these particular transitions, which involve configurations from other shells.

Figure 7 also shows the sensitivity of the  $A_y$  values to the choice of phase. There is a clear choice

TABLE I. Spectroscopic information from the  $^{106}\text{Pd}(\vec{t}, \alpha)^{105}\text{Rh}$  reaction experiments.

Group No. <sup>a</sup>	Present results			Previous measurements <sup>c</sup>	
	$E_x^b$ (keV)	$J^\pi$	$C^2S$	$E_x$ (keV)	$J^\pi$
0	0	$\frac{7}{2}^+$	(0.21)	0	$\frac{7}{2}^+$
1	$133 \pm 5$	$\frac{1}{2}^-$	1.6	129.6	$\frac{1}{2}^-$
2	$152 \pm 5$	$\frac{9}{2}^+$	4.1	149.2	$(\frac{9}{2})^+$
3	$\equiv 392.5$	$\frac{3}{2}^-$	0.66	392.5	$\frac{3}{2}^-$
4	$455 \pm 5$	$\frac{5}{2}^-$	0.23	455.5	$(\frac{5}{2}, \frac{3}{2})^-$
				469.3	$(\frac{3}{2})^+$
				474 <sup>e</sup>	$(\frac{9}{2}^+, \frac{7}{2}^+)$
5	$498 \pm 5$	$\frac{5}{2}^+$		499.3	$\frac{5}{2}^+$
				524 <sup>e</sup>	
				638.6	$(\frac{7}{2}^+)$
6	$722 \pm 5$	$\frac{3}{2}^- - (\frac{5}{2}^+)$		724.3	$\frac{5}{2}^+$
7	$759 \pm 5$	$\frac{3}{2}^-$	1.3	762.0	$(\frac{3}{2}^+)$
				783 <sup>e</sup>	$(\frac{1}{2}, \frac{3}{2})^-$
				785.8	$(\frac{5}{2}^-)$
				805.8	$\frac{3}{2}^+$
				817 <sup>e</sup>	
8	$830 \pm 8$	$\frac{9}{2}^+$	1.3	833 <sup>e</sup>	
				858 <sup>e</sup>	$(\frac{3}{2}^-, \frac{1}{2}^-)$
9	$866 \pm 8$	$\frac{5}{2}^-$	2.8	868 <sup>e</sup>	$(\frac{5}{2}, \frac{3}{2})^-$
				898 <sup>e</sup>	$(\frac{7}{2})^-$
				924 <sup>e</sup>	
				969.4	$\frac{5}{2}^+$
				976	$(\frac{9}{2}, \frac{7}{2})^-$
10	$1024 \pm 8$	$(\frac{7}{2}^+)$	(0.45)		
11	$1143 \pm 8$			1147 <sup>f</sup>	$(\frac{3}{2}, \frac{5}{2})^-$
				1190 <sup>e</sup>	
				1215 <sup>f</sup>	$(\frac{3}{2}, \frac{5}{2})^-$
12	$1295 \pm 8$	$\frac{1}{2}^-$	0.21	1297 <sup>f</sup>	$\frac{1}{2}^-$
				1321.3	$(\frac{5}{2}^+)$
13	$1327 \pm 20^d$			1345.2	$(\frac{3}{2}^+)$
				1351 <sup>f</sup>	$(\frac{3}{2}, \frac{5}{2})^-$
				1377.0	$(\frac{3}{2}^+, \frac{5}{2})$
				1393 <sup>e</sup>	
				1441.3	$(\frac{3}{2}^+, \frac{5}{2})$

TABLE I. (Continued.)

Group No. <sup>a</sup>	Present results		Previous measurements <sup>c</sup>		
	$E_x^b$ (keV)	$J^\pi$	$C^2S$	$E_x$ (keV)	$J^\pi$
14	$1462 \pm 10$	$\frac{3}{2}^-$		1463 <sup>f</sup>	$(\frac{3}{2}, \frac{5}{2})^-$
				1486.7	$(\frac{3}{2}, \frac{5}{2})^-$
				1521 <sup>e</sup>	$(\frac{5}{2}^-, \frac{7}{2}^-)$
				1577 <sup>e</sup>	
15	$1608 \pm 8$			1649 <sup>f</sup>	$(\frac{3}{2}, \frac{5}{2})^-$
16	$1684 \pm 8^d$			1690 <sup>f</sup>	
				1698.3	$(\frac{3}{2}^+, \frac{5}{2})$
				1708.4	$(\frac{3}{2}^+, \frac{5}{2})$
				1721.3	$(\frac{5}{2}^+)$
17	$1750 \pm 12$			1758 <sup>f</sup>	$(\frac{7}{2}, \frac{9}{2})^-$
				1765.4	$(\frac{5}{2}^+, \frac{3}{2}^+)$
				1809.7	$(\frac{5}{2}, \frac{3}{2}^+)$
18	$1832 \pm 10^d$			1829.6	$(\frac{5}{2}, \frac{3}{2}^+)$
				1849 <sup>f</sup>	$(\frac{3}{2}, \frac{5}{2})^-$
				1864 <sup>e</sup>	
19	$1889 \pm 10$			1887 <sup>f</sup>	$(\frac{3}{2}, \frac{5}{2})^-$
				1904 <sup>f</sup>	
				1913 <sup>e</sup>	$(\frac{3}{2}^+, \frac{5}{2}^+)$
20	$1942 \pm 10$			1936 <sup>f</sup>	$(\frac{7}{2}, \frac{9}{2})^-$
				1957 <sup>e</sup>	
21	$2001 \pm 10$			2005 <sup>f</sup>	$(\frac{7}{2}, \frac{9}{2})^-$
				2033 <sup>f</sup>	$(\frac{7}{2}, \frac{9}{2})^-$
22	$2041 \pm 15$			2061 <sup>f</sup>	$(\frac{7}{2}, \frac{9}{2})^-$
				2083 <sup>f</sup>	$(\frac{7}{2}, \frac{9}{2})^-$
23	$2075 \pm 10^d$			2109 <sup>f</sup>	$(\frac{7}{2}, \frac{9}{2})^-$
24	$2113 \pm 10^d$				

<sup>a</sup>See Figs. 1 and 4.<sup>b</sup> $E_x$  relative to the third excited state whose  $E_x$  is taken to be 392.5 keV.<sup>c</sup>See Y. A. Ellis, Nucl. Data Sheets 27, 1 (1979). Uncertain states are not shown here.<sup>d</sup>This group appears to correspond to unresolved states.<sup>e</sup> $\pm 5$  keV.<sup>f</sup> $\pm 10$  keV.

of an opposite  $\frac{7}{2}^- - \frac{9}{2}^-$  phase (solid line) over the same phase (dashed line), indicating that the  $A_y$  results are valuable in helping to select the correct phase of the wave function, which here is considered as a mixture of single-particle and particle-vibration components. The shapes of the cross sections are very similar in the two cases and do not permit this phase deter-

mination. The shapes of  $A_y$  from the CCBA calculations are not very different from the DWBA results shown in Figs. 4 and 5. Similar results occur for the  $\frac{5}{2}^+$  states, as indicated in Fig. 8. Here the agreement with the data is even more remarkable, and again the choice of phases is clearly that of opposite sign between  $\frac{9}{2}^+$  and  $\frac{5}{2}^+$  transfers.

TABLE II. Spectroscopic information from the  $^{108}\text{Pd}(\vec{t}, \alpha)^{107}\text{Rh}$  reaction experiments.

Group No. <sup>a</sup>	Present results		$C^2S$	Previous measurements <sup>c</sup>	
	$E_x^b$ (keV)	$J^\pi$		$E_x$ (keV)	$J^\pi$
0	0	$\frac{7}{2}^+, (\frac{5}{2}^-)$	(0.26)	0	$(\frac{7}{2}^+)$
1	$\equiv 194.1$	$\frac{9}{2}^+$	4.0	194.1	$(\frac{9}{2}^+)$
2	$268 \pm 3$	$\frac{1}{2}^-$	1.4	$280 \pm 20$	$(\frac{1}{2}^-)$
				405.9	
3	$464 \pm 5$	$(\frac{5}{2}^+)$		462.6	
4	$488 \pm 3$	$(\frac{3}{2}^-)$	(0.72)		
				568.5	
				683.5	
5	$754 \pm 5$	$\frac{3}{2}^-$	2.0	$750 \pm 20$	$(\frac{3}{2}^-)$
6	$878 \pm 5$	$\frac{5}{2}^-$	3.3		
7	$914 \pm 5^d$			912.0	
8	$969 \pm 8^d$	$(\frac{5}{2}^-)$			
9	$1006 \pm 5$	$\frac{9}{2}^+$	2.3		
				1042.0	$(\frac{7}{2}^+)$
10	$1252 \pm 8$			1272.2	
				1306.3	
11	$1341 \pm 8$				
12	$1371 \pm 8^d$			$1360 \pm 20$	$(\frac{7}{2}^+, \frac{9}{2}^+)$
13	$1548 \pm 8$	$\frac{3}{2}^-$	0.48	$1570 \pm 20$	
14	$1632 \pm 8$				
15	$1669 \pm 8^d$				
16	$1701 \pm 8$	$(\frac{5}{2}, \frac{9}{2})^+$		$1720 \pm 20$	$(\frac{1}{2}^-, \frac{3}{2}^-)$
17	$1865 \pm 8$	$\frac{3}{2}^-$	0.20		
18	$1931 \pm 10^d$				
19	$2037 \pm 8$	$\frac{5}{2}^-$	0.93		
20	$2201 \pm 8$				

<sup>a</sup>See Figs. 2 and 5.<sup>b</sup> $E_x$  relative to the first excited state whose  $E_x$  is taken to be 194.1 keV.<sup>c</sup>B. Harmatz, Nucl. Data Sheets **34**, 643 (1981).<sup>d</sup>This group appears to correspond to unresolved states.

## V. DISCUSSION

The use of the  $(\vec{t}, \alpha)$  reaction in the spectroscopy of proton hole states is clearly illustrated by the assignment of spin and spectroscopic values in Tables I and II. From these data and those of Ref. 1, we are able to examine the systematics of such states in the Rh nuclei and compare the results with known data on the Tc isotopes (see Fig. 6 of Ref. 1) and Nb isotopes.<sup>12</sup>

Figure 9 is a presentation of the lower levels of all

Rh isotopes between  $A=99$  ( $N=54$ ) and  $A=109$  ( $N=64$ ). The ground state spin is  $\frac{1}{2}^-$  for the lighter nuclei, changing to  $\frac{7}{2}^+$  at  $^{105}\text{Rh}$ . This change occurs between  $N=58$  and 60, the latter neutron number being associated with an onset of deformation. This transition to deformation is particularly rapid in  $^{98}\text{Zr} \rightarrow ^{100}\text{Zr}$  and becomes more gradual with increasing  $Z$  [see Ref. 6 for the  $\text{Mo}(t, p)$  systematics]. In Table III we present the strong proton-hole states observed here and in Ref. 1. From this table and Fig. 9, we note that the excitation energy and

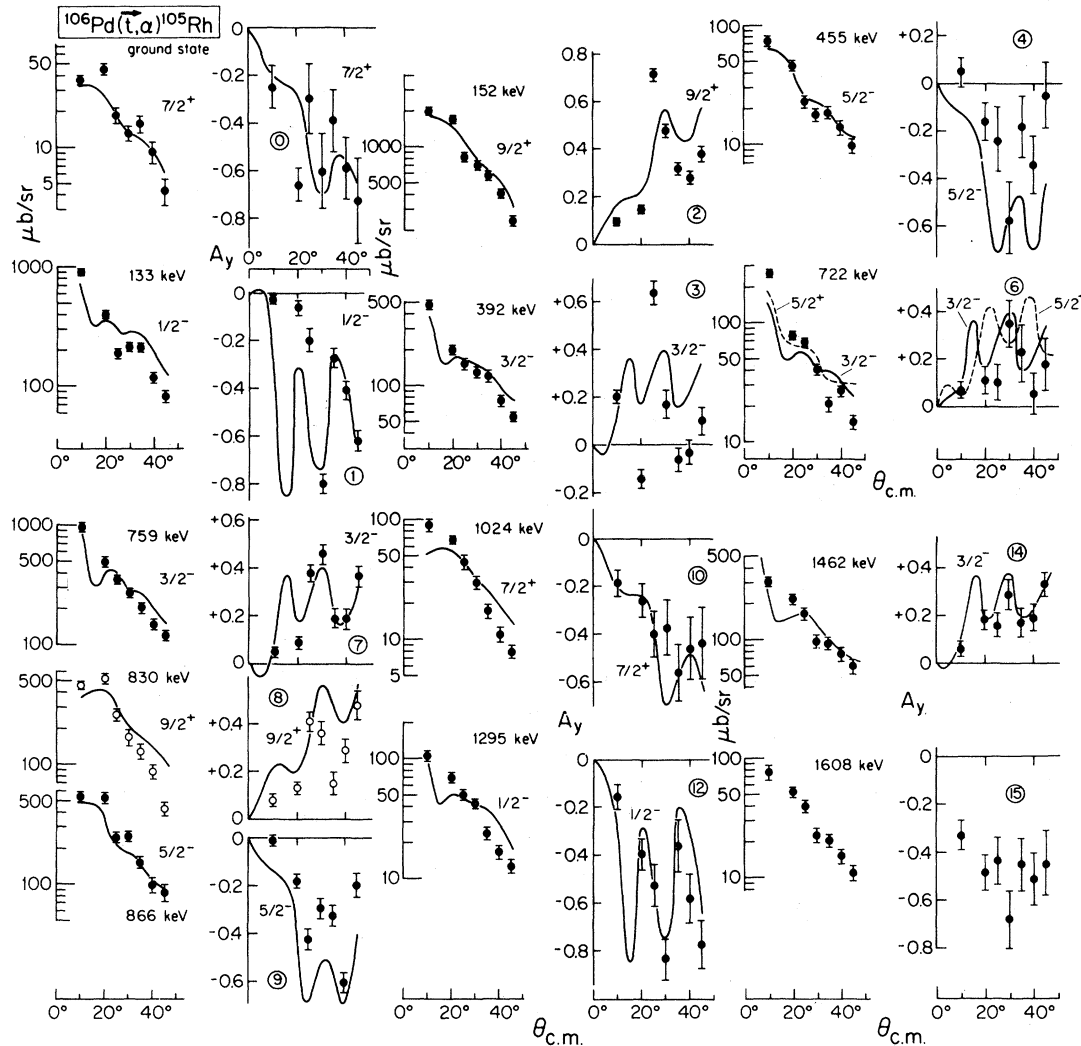


FIG. 4. Differential cross sections and analyzing powers for the  $^{106}\text{Pd}(\vec{t}, \alpha)$  reaction. The solid lines are DW calculations.

strength of the  $\frac{9}{2}^+$ ,  $\frac{3}{2}^-$ , and  $\frac{5}{2}^-$  levels are remarkably uniform throughout the heavier isotopes measured here. Indeed, the excitation energy of the  $\frac{9}{2}^+$  state, which has been observed all the way down to  $A=99$ , does not change appreciably. The  $\frac{1}{2}^-$  state shows a gradual tendency to rise in excitation energy with increasing neutron number.

It has been proposed<sup>4</sup> that a strong isospin interaction may occur in this nuclear region between the filling  $g_{7/2}$  neutron and the  $g_{9/2}$  proton orbitals. Similar effects may be expected with subsequent  $h$  particles. This effect may explain the presence of the  $\frac{7}{2}^+$  state as a ground state in the heavier Rh isotopes. In  $^{96}\text{Zr}$  there is strong evidence<sup>6</sup> for a subshell closure of the  $d_{5/2}$  shell at  $N=56$ . This is reflected in a definite shift in proton levels in the Nb

isotopes at  $^{97}\text{Nb}$ , the  $N=56$  nucleus. At higher neutron numbers the  $s_{1/2}$ ,  $d_{3/2}$ , and  $g_{7/2}$  orbitals begin to fill. However, in the systematics of Fig. 9, this subshell effect is quite small in  $^{101}\text{Rh}$ , although a 100 keV perturbation in the  $g_{9/2}$  level is seen. (In  $^{97}\text{Nb}$ , a shift of 500 keV in the splitting between the  $p_{1/2}$  and  $g_{9/2}$  proton orbitals is observed as compared to adjacent odd  $A$  Nb isotopes). This indicates that in Rh the  $N=56$  subshell gap has mostly disappeared, and that the  $g_{7/2}$  neutron orbitals are filling earlier. Thus the more slowly varying behavior for the proton states as a function of neutron number indicates a very mixed neutron configuration in the Rh isotopes.

The behavior of the Rh isotopes also differs substantially from the Tc isotopes, which have just two

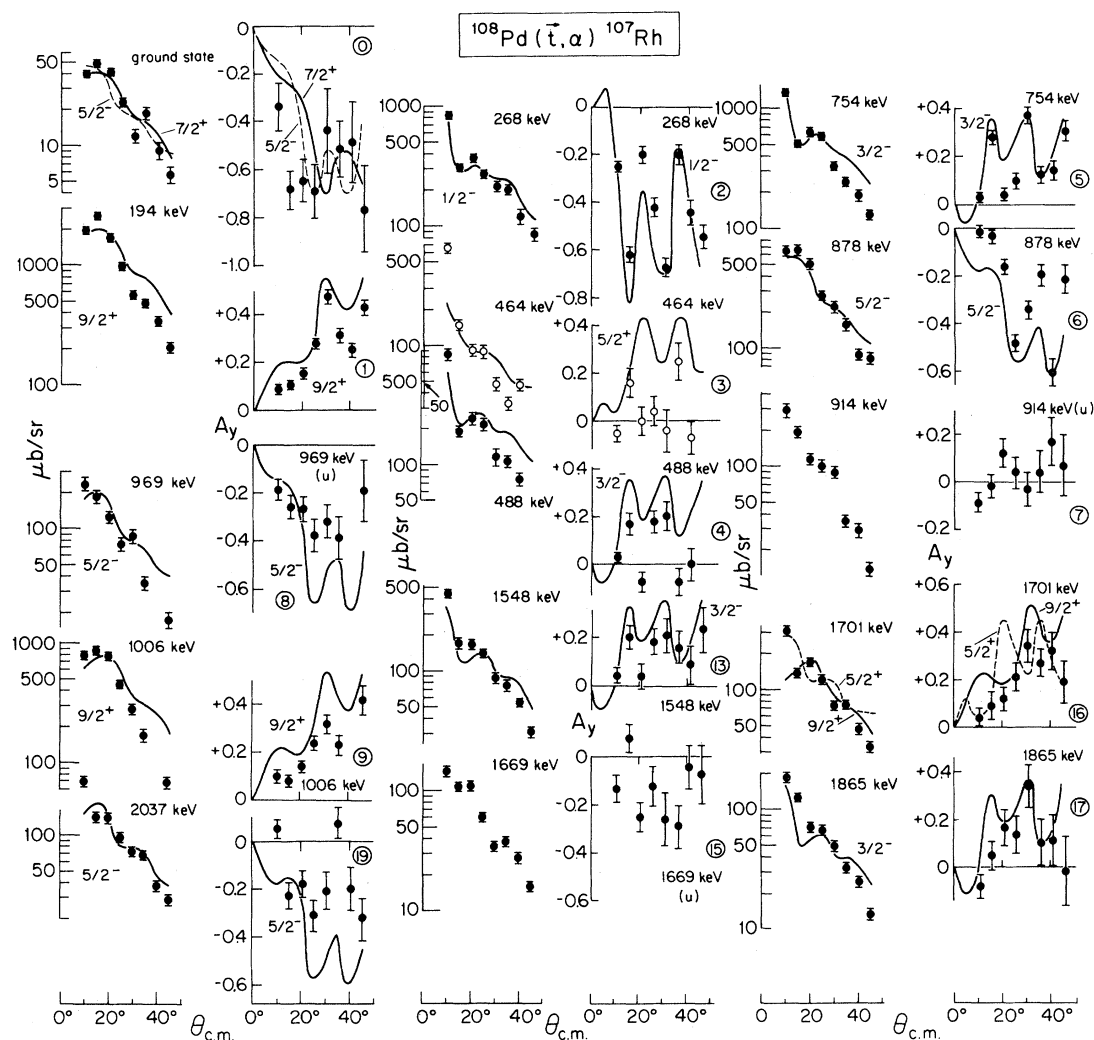


FIG. 5. Differential cross sections and analyzing powers for the  $^{108}\text{Pd}(\vec{t}, \alpha)$  reaction. The solid lines are DW calculations. Groups labeled (u) may be due to unresolved states.

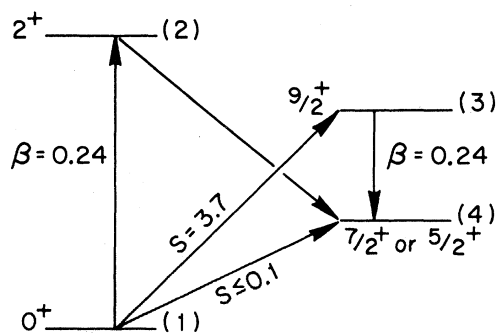


FIG. 6. Channel couplings in the CCBA calculation for the  $\frac{7}{2}^+$  or  $\frac{5}{2}^+$  states of the Rh isotopes. The numbers in parentheses are the channel numbers.

protons less. In Fig. 6 of Ref. 1, a much more rapid rearrangement of proton orbitals as a function of neutron number is observed. The  $\frac{3}{2}^-$  and  $\frac{5}{2}^-$  single particle states, which are seen here to be relatively stable in energy as a function of neutron number, drop rapidly in Tc with increasing  $N$ . In the Rh isotopes the states carrying the primary strength for these two orbitals remain constant in excitation energy at approximately 800 keV. In Tc these orbitals drop from 600 keV at  $N=54$  to  $\sim 150$  keV at  $N=60$ . The latter case is thus 650 keV below the corresponding  $N=60$  nucleus,  $^{103}\text{Rh}$ . In Tc there is also a rearrangement of orbitals as  $N$  is increased until, at  $^{103}\text{Tc}$ , there appears to develop a level sequence strongly reminiscent of deformed orbital spacing. Thus, again the evidence is that the transi-



TABLE III. A summary of the dominant proton-hole states observed in the  $\text{Pd}(t,\alpha)\text{Rh}$  reactions.

Residual $A=$	109		107		105	
$J^\pi$	$E_x$ (keV)	$C^2S$	$E_x$ (keV)	$C^2S$	$E_x$ (keV)	$C^2S$
$\frac{9}{2}^-$	206	3.7	194	4.0	152	4.1
$\frac{1}{2}^-$	374	1.4	268	1.4	133	1.6
$\frac{3}{2}^-$	737	1.7	754	2.0	759	1.3
$\frac{5}{2}^-$	852	2.3	878	3.3	866	2.8

tional character of nuclei in this region is a strong function of proton number. Certainly there is a much more gradual tendency toward deformation in Rh than in Tc, and shell effects such as those seen in Nb are almost completely gone.

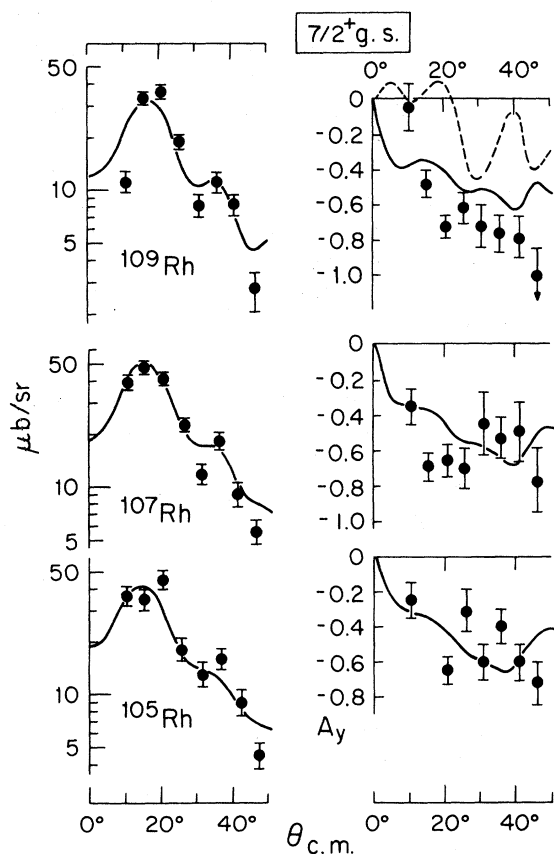


FIG. 7. Comparison of CCBA calculations with the data for the  $\frac{7}{2}^+$  ground states. The solid line is for an opposite relative phase between the  $\frac{7}{2}^+$  and  $\frac{9}{2}^+$  single particle transfer. The dashed line for  $A_y$  in the case of  $^{109}\text{Rh}$  is for identical phases. In this case the shapes of  $d\sigma/d\Omega$  are very similar.

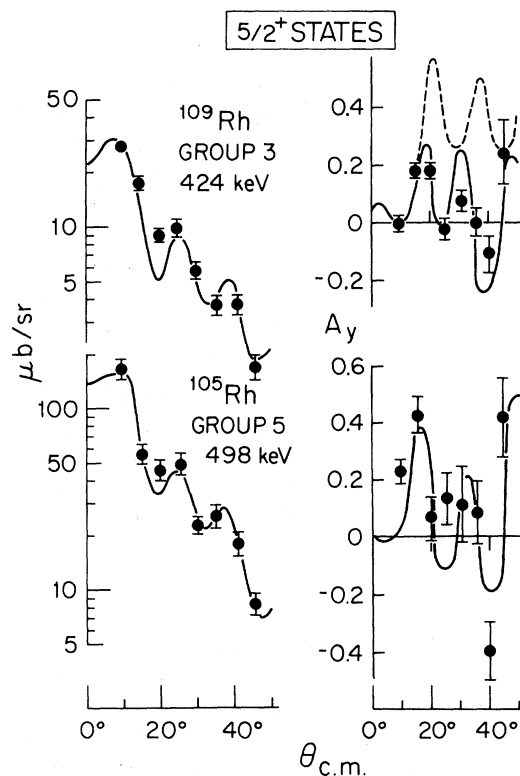


FIG. 8. Comparison of CCBA results with the data for the lowest  $\frac{5}{2}^+$  states in  $^{105,109}\text{Rh}$ . See also the caption of Fig. 7.

The present results also offer a comparison to the particle-vibration model in the case of  $^{105}\text{Rh}$ , where previous  $^{103}\text{Rh}(t,p)^{105}\text{Rh}$  data exist.<sup>7</sup> The  $\frac{3}{2}^- - \frac{5}{2}^-$  doublet at 392–455 keV represents a particle-vibration multiplet based on the  $2^+$  state of the  $^{104}\text{Ru}$  (or  $^{106}\text{Pd}$ ) core at  $\sim 390$  keV (or  $\sim 510$  keV). These two levels have a  $(t,p)$  cross-section ratio that reasonably agrees with the  $(2J+1)$  rule and have the total cross section expected of a multiplet of the form

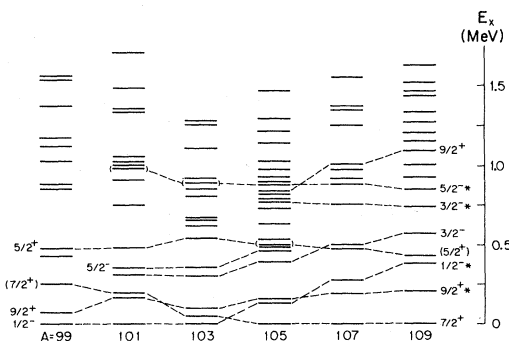


FIG. 9. The low lying states of all known Rh isotopes. The asterisks designate the principal single hole states.

$$[^{104}\text{Ru} (2_1^+) \times \frac{1}{2}^-]_{3/2^-, 5/2^-}$$

However, the centroid lies lower than a simple weak coupling picture would suggest. The ground state and  $\frac{9}{2}^+$  states of  $^{105}\text{Rh}$  are not excited in the  $(t, p)$  reaction, indicating their lack of parentage in the Pd or Ru negative parity vibrational states. In the current experiment, the  $\frac{3}{2}^-$  state of the doublet shows strong single-particle mixing with the 759 keV  $\frac{3}{2}^-$  state and contains about one-half of the strength of the latter state. The  $\frac{5}{2}^-$  state is much less strongly mixed with the 866-keV  $\frac{5}{2}^-$  state, containing less than 10% of the strength of the latter state, and it is not even populated in the heavier isotopes. This is consistent with  $(^3\text{He}, d)$  studies of  $^{105}\text{Rh}$ , which also excites the  $\frac{3}{2}^-$ , but not the  $\frac{5}{2}^-$  state.<sup>13</sup> The next doublet which was considered in the  $(t, p)$  studies is the

$$[^{104}\text{Ru} (2_2^+) \times \frac{1}{2}^-]_{3/2^-, 5/2^-}$$

at 759 and 866 keV, which contains the dominant  $f_{5/2}$  single particle state; thus this description must be regarded with some suspicion, although a similar situation does exist in the Tl isotopes.<sup>3</sup> A doublet at 896 and 976 keV arising from coupling to the  $4^+$  state is not seen in the present experiment. Since the spin of these states is  $\frac{7}{2}^-$  and  $\frac{9}{2}^-$ , this is reasonable, as there should be no single particle components. The  $\frac{1}{2}^-$  state at 1295 keV seen in the  $(t, p)$  work is confirmed by the present data. The combination of the  $(t, \alpha)$  results with the  $(t, p)$  data should make more extensive particle-vibration studies more rewarding. In particular, the approach used by Paar<sup>14</sup> to understand the nuclei with three protons outside a closed shell, if extended to the five particle configuration, could be applied to the Rh nuclei.

An alternative approach to understanding the

particle-vibration character of the positive parity excitations in the Rh nuclei may lie in the interacting boson fermion approximation (IBFA) model.<sup>15</sup> The low-lying vibrational states in the Ru and Pd cores have been studied extensively.<sup>16</sup> It would be of interest to see if the ordering of the positive parity states in the odd  $Z$  nuclei could be understood in the framework of the IBFA, or if an explicit neutron-proton interaction must be included.

As a final comment on particle-vibration multiplets, we consider the CCBA calculations performed on the low-lying  $\frac{7}{2}^+$  and  $\frac{5}{2}^+$  states in  $^{105, 107, 109}\text{Rh}$ . The magnitude and shape of  $d\sigma/d\Omega$  were reasonably reproduced for the  $\frac{7}{2}^+$  states in these calculations, as well as the shapes of  $A_y$ . This was done using known  $2^+$  energies and  $\beta$  values for the Pd system. These  $\frac{7}{2}^+$  and  $\frac{5}{2}^+$  states are very weakly populated, and the arguments here only indicate that the two-step mechanism of the CCBA may be responsible. However, the  $g_{7/2}$  orbital lies directly above the shell being investigated, with the  $d_{5/2}$  orbital somewhat higher. Thus small amounts of single particle admixtures may occur in these  $\frac{7}{2}^+$  states. The present data and calculation strongly support the argument that the presence of the  $\frac{7}{2}^+$  state as a ground state is in all likelihood due to strong core coupling. In addition, the  $A_y$  results suggest the correct relative phase between the core coupled and single particle components. We note that other multiplets which contain no single particle components such as the  $[4^+ \times \frac{1}{2}^-]_{7/2^-, 9/2^-}$  are not seen.

The authors are grateful to S. Orbesen for his help with the Q3D, to the crew of the Van de Graaff facility for their help with the polarized triton beam, and to Judy Gursky who prepared the targets. This work was supported by the United States Department of Energy.

\*Permanent address: Department of Physics, University of Pennsylvania, Philadelphia, Pennsylvania 19104.

†Present address: A. W. Wright Nuclear Structure Laboratory, Yale University, New Haven, Connecticut 06511.

<sup>1</sup>E. R. Flynn, F. Ajzenberg-Selove, R. E. Brown, J. A. Cizewski, and J. W. Sunier, Phys. Rev. C **24**, 902 (1981); **25**, 2851(E) (1982).

<sup>2</sup>O. Straume, G. Lovhøiden, D. G. Burke, E. R. Flynn, and J. W. Sunier, Z. Phys. A **293**, 75 (1979).

<sup>3</sup>E. R. Flynn, R. A. Hardekopf, J. D. Sherman, J. W. Sunier, and J. P. Coffin, Nucl. Phys. A **279**, 394 (1977).

<sup>4</sup>P. Federman and S. Pittel, Phys. Rev. C **20**, 820 (1979).

<sup>5</sup>K. Sistemich, W. D. Lauppe, H. Lawin, H. Seyforth, and B. D. Kern, Z. Phys. A **289**, 225 (1979).

<sup>6</sup>E. R. Flynn, F. Ajzenberg-Selove, R. E. Brown, J. A. Cizewski, and J. W. Sunier, Phys. Rev. C **24**, 2475 (1981); **25**, 2850(E) (1982).

<sup>7</sup>R. E. Anderson, J. J. Kraushaar, I. C. Oelrich, R. M. Del Vecchio, R. A. Naumann, E. R. Flynn, and C. E. Moss, Phys. Rev. C **15**, 123 (1977).

<sup>8</sup>Table of Isotopes, 7th ed., edited by C. M. Lederer and V. S. Shirley (Wiley, New York, 1978).

<sup>9</sup>E. R. Flynn, S. D. Orbesen, J. D. Sherman, J. W. Sunier, and R. Woods, Nucl. Instrum. Methods **128**, 35 (1975).

<sup>10</sup>P. D. Kunz, code DWUCK4 (unpublished).

<sup>11</sup>P. D. Kunz, code DWUCK5 (unpublished).

<sup>12</sup>E. R. Flynn, R. E. Brown, F. Ajzenberg-Selove, and J. A. Cizewski, Phys. Rev. C (to be published).

<sup>13</sup>D. L. Dittmer and W. W. Daehnick, Phys. Rev. C 2, 238 (1970).

<sup>14</sup>V. Paar, Nucl. Phys. A211, 29 (1973).

<sup>15</sup>F. Iachello and O. Scholten, Phys. Rev. Lett. 43, 679 (1979).

<sup>16</sup>P. Van Isacker and G. Puddu, Nucl. Phys. A348, 125 (1980).